Forest Dragon 2: Final results of the European partners

Schmullius, Christiane ; Leiterer, Reik ; Santoro, Maurizio ; Burjack, Ina ; Traut, Kerstin ; Li, Zengyuan ; Ling, Feilong

Abstract: The European contribution to the Forest DRAGON 2 focused on the evaluation of multi-temporal, multi-sensor and multi-scale Earth Observation images and data products within the vegetation ecosystem of Northeast China. The forest growing stock volume (GSV) map produced with ERS-1/2 coherence images for 1995-1998 and two GSV maps produced from Envisat ASAR ScanSAR data for 2005 and 2010 were inter-compared with respect to several datasets (in situ, EO images and EO data products) to assess the plausibility of the GSV estimates, the contribution to land cover mapping and the dynamics over time. For this purpose, a multi-source database was set up including in situ data and EO data products. Land use / land cover (LULC) datasets identified mis-classification of GSV in the ERS dataset primarily for cropland. An a posteriori correction of the GSV resulted in an increase of overall accuracy up to 7%. LULC products can also support the fine tuning of the algorithm to estimate GSV from ASAR data particularly in transition regions between forest and shrubland. The ASAR-based GSV estimates were consistent and highlighted areas of change. From the two ASAR maps, slight loss of volume from 2005 to 2010 was estimated.

Originally published at:
Schmullius, Christiane; Leiterer, Reik; Santoro, Maurizio; Burjack, Ina; Traut, Kerstin; Li, Zengyuan; Ling, Feilong (2012). Forest Dragon 2: Final results of the European partners. In: Dragon 2 Final Results Dragon 3 Kick-Off Symposium, Beijing, China, 25 June 2012 - 29 June 2012. European Space Agency * Communication Production Office, online.

FOREST DRAGON 2: FINAL RESULTS OF THE EUROPEAN PARTNERS

C. Schmullius[(1)], R. Leiterer [(1)], I. Burjack[(1)], K. Traut[(1)], M. Santoro[(3)], Z.Y. Li[(3)], F.L. Ling[(3)],

[(1)] Department of Earth Observation, Friedrich-Schiller University Jena, Grietgasse 6, 07745 Jena, Germany;
Email: c.schmullius@uni-jena.de. reik.leiterer@geo.uzh.ch, ina.burjack@uni-jena.de, kerstin.traut@uni-jena.de
[(2)] Gamma Remote Sensing, Worbstrasse 225, 3073 Gümligen, Switzerland;
Email: santoro@gamma-rs.ch
[(3)] Forest Remote Sensing Lab, Research Institute of Forest Resource Information Techniques, Chinese Academy of Forestry , Wanshoushan Hou, Haidian, 1000091 Beijing, China;
Email: zengyuan.li@caf.ac.cn, lfl@fzu.edu.cn

ABSTRACT

The European contribution to the Forest DRAGON 2 focused on the evaluation of multi-temporal, multi-sensor and multi-scale Earth Observation images and data products within the vegetation ecosystem of Northeast China. The forest growing stock volume (GSV) map produced with ERS-1/2 coherence images for 1995-1998 and two GSV maps produced from Envisat ASAR ScanSAR data for 2005 and 2010 were inter-compared with respect to several datasets (in situ, EO images and EO data products) to assess the plausibility of the GSV estimates, the contribution to land cover mapping and the dynamics over time. For this purpose, a multi-source database was set up including in situ data and EO data products. Land use / land cover (LULC) datasets identified mis-classification of GSV in the ERS dataset primarily for cropland. An a posteriori correction of the GSV resulted in an increase of overall accuracy up to 7%. LULC products can also support the fine tuning of the algorithm to estimate GSV from ASAR data particularly in transition regions between forest and shrubland. The ASAR-based GSV estimates were consistent and highlighted areas of change. From the two ASAR maps, slight loss of volume from 2005 to 2010 was estimated.

1. INTRODUCTION

The Forest DRAGON Project within the DRAGON-1 and DRAGON-2 Programmes has as objectives the monitoring of the forest ecosystem of China by means of multi-source Earth Observation (EO) data. At the end of the DRAGON-2 Programme, a huge archive of satellite synthetic aperture radar (SAR) imagery spanning the last 17 years has been collected. European Remote Sensing (ERS) data acquired between 1995 and 1998 were used to map four classes of forest growing stock volume (GSV) in Northeast and South China at 50 m spatial resolution [1-3]. An update of the GSV with Envisat ASAR Stripmap images acquired during 2004 and 2005 was attempted but did not produce sufficiently accurate results; for this reason it was preferred to assess changes with respect to the mid-1990s baseline in form of forest/non-forest cover [4]. The availability of extensive datasets of Envisat ASAR ScanSAR images over China since 2004 favoured the retrieval of GSV using the BIOMASAR approach proposed in [5]. A first attempt of using the BIOMASAR algorithm for a site in Northeast China showed that the GSV estimates presented certain agreement with the MODIS Vegetation Continuous Field tree canopy cover estimates [2]. The BIOMASAR algorithm has been applied to Northeast China to provide estimates of GSV for the years 2005 and 2010. Assessment of the ERS and Envisat ASAR ScanSAR GSV datasets over Northeast China has been pursued in the second half of the Forest DRAGON-2 project. For this, several data pools have been collected and merged into a geoportal (Section 2). Land use / land cover (LULC) products have been used to assess the thematic plausibility of the GSV estimates (Section 3). EO products have been used to confirm detected changes of GSV estimates between the two epochs of the Envisat ASAR ScanSAR data used for the GSV retrieval (2005 and 2010), The ASAR-based GSV maps have then been used to provide overall statistics of forest volume changes in Northeast China between 2005 and 2010 (Section 4).

2. FOREST DRAGON GEOPORTAL

The lack of extensive forest inventory data has hindered thorough validation of the SAR based DRAGON GSV products so far. To support validation activities or, at least, to verify the quality of the SAR-based GSV maps, a multi-source database was set up including in situ data, various open-source and intra-project EO-based datasets of GSV, vegetation cover and several forest and land parameters. The multi-source database was initially prepared in ArcGIS 10.0 and further translated into a geoportal.

Table 1. Datasets included in the Forest DRAGON geoportal.

Category	Dataset	Data type	Source
Forest DRAGON Products	ERS-1/2 GSV map 1995 based on tandem coherence	raster, continuous	[1]
	ASAR GSV map 2005 based on BIOMASAR algorithm	raster, continuous	[5]
Growing Stock Volume Data	Field Campaign Data 2011	vector, point	
	Literature Databases	vector, point	[6]
	Forest Ecosystem Database	vector, point	[7]
	Provincial Data	vector, polygon	[8]
	IIASA GSV map 2005	raster, continuous	[9]
EO datasets, forest-related	Forest Canopy Height 2005	raster, continuous	[10]
	MODIS NDVI (multiple years / multiple spatial resolutions)	raster, continuous	[11]
	MODIS Active Fire (multiple years)	vector, point	[12]
	ATSR World Fire Atlas (multiple years)	vector, point	[13]
	MODIS Burned Area (multiple years)	vector, point	[14]
Land Cover Data	MODIS VCF Percent Tree Cover (multiple years / multiple spatial resolutions)	raster, continuous	[15, 16]
	Panarctic Vegetation Cover	raster, continuous	[17]
	GLC2000	raster, categories	[18]
	MODIS Land Cover 2005	raster, categories	[19]
Photo Libraries	Field Campaign Photos 2011	vector, point	
	Confluence Points	vector, point	[20]
	Field Campaign Photos (University of Oklahoma)	vector, point	[21]
Other EO datasets	SRTM DEM 2000	raster, continuous	[22]
	Landsat Surface Reflectance (multiple years)	raster, continuous	[23]

A summary of all datasets implemented in the geoportal by the end of the DRAGON 2 programme is given in Table 1. The layer structure of the geoportal can be taken from the category column.

The GSV database was built-up based on in situ measurements and values reported in literature [6-8]. Field inventory data were collected at selected test sites in Northeast China in September 2011. For the GSV derivation, pointwise measurements of diameter at breast height (DBH) and tree height were converted to GSV values by using species-dependent allometric equations. A pointwise measurement here means that within a radius of 20 m the DBH of all trees and the height of 15 representative trees has been estimated and averaged for each circular area. GSV values were stored for the centre coordinates in a point dataset. In total, 12 plots were visited and measured.

GSV measurements reported in literature were first screened to check whether information on precise coordinates of the inventory location, the date of the inventory, GSV or biomass values as well as the formula for GSV calculation was documented. Values that satisfied the criteria above were tentatively included in the database. In most cases, GSV was expressed by different synonyms (e.g., stem volume, forest volume, volume of standing stock) or had to be calculated from other forest parameters (e.g., biomass, biomass density, biomass expansion factors). For the literature database [6] and the forest ecosystem database [7], uncertainties remained concerning the precision of the geographic coordinates and accuracies of the GSV values. For this, the data were checked in Google Earth. In this process each point was sorted into one of the three classes:
1. potentially correct inventory information,
2. potential land cover change between time of inventory and time of evaluation or
3. incorrect inventory indication.

All points that have shown consistency between the specifications found in literature and the information in Google Earth were retained in the final database.

The geoportal includes several freely available EO images or EO-based data products related to forestry and land cover. MODIS NDVI refers to monthly averages of differently spatially resolved (250m, 500m and 1000m) 16-day MODIS NDVI composites for the year 2005 [11]. As elevation dataset, the SRTM DEM with 3-arcseconds spatial resolution is used [22].

The geoportal includes an extensive photo library with over 300 points of georeferenced pictures of forest appearance for the areas visited during the field trip in Northeast China during September 2011. Other photo libraries for Northeast China were built-up on the basis of a Global Geo-Referenced Field Photo Library - a

Web-based data portal designed by University of Oklahoma for researchers who wish to archive and share field photos [21] and selected pictures of the Degree Confluence Project, a Web-based project which aims to have photographs of each of the integer degree intersections of latitude and longitude worldwide [20].

Preparatory steps for all datasets included harmonization processes relating to geographical projection (Lat/Long, WGS84), adaption of no data values (NaNs) and the extraction of dataset specific study areas in ArcGIS 10.0. The datasets listed in Table 1 were summarized in an ArcGIS project and further translated into the geoportal. Raster data were stored in GeoTiff format and vector data (points and polygons) as Shape-files.

The basis of the Forest DRAGON geoportal is formed by the GeoServer, which is a Java written open source software server that facilitates users to provide geospatial data in an OGC (Open Geospatial Consortium) compliant form. The OGC WMS (Web Map Service) standard allows the integration of the datasets into other portals as well as Desktop-GIS Software like for instance ArcGIS or Quantum GIS [24]. The geoportal frontend is based on the open-source JavaScript libraries Openlayers, MapQuery and jQuery. The background is formed by the three Google Maps layout types "Satellite", "Hybrid" and "Terrain" as well as two OpenStreetMap datasets. To keep an unique appearance, the primary layout is leaned to other geoportal designs created by the Department of Earth Observation of FSU Jena. The color scheme of each dataset was assigned by a layer specific Styled Layer Descriptor (SLD), a XML scheme defined by the OGC.

The Forest DRAGON geoportal is accessible through the Forest DRAGON 2 homepage of FSU Jena (http://www.forestdragon2.uni-jena.de/geoportal). All layers in the geoportal are publically available for viewing only. Download of data is restricted to registered users.

3. SYNERGY OF GSV AND LULC PRODUCTS

The SAR-based GSV products show the spatial distribution of a bio-physical variable. To link a biophysical variable such as GSV to a discrete land cover classification, the potential and the uncertainties of a synergistic usage had to be investigated first.

For this purpose, six freely available global LULC products were used. The LULC products have been chosen so that different global products were available for the inter-comparison with the ERS-1/2 and the Envisat ASAR GSV products (Table 2). The LULC products were grouped according to the time period of acquisition of the images used for their derivation. This resulted in three groups related respectively to the time period of 1992-1993, 1999-2001 and 2004-2006. A more detailed description of each dataset is given in [2].

For generating a consistent basis for the inter-comparison, we concentrated on four main target classes: forest, cropland, other vegetation und non-vegetation. These are especially significant for environmental modelling. The method used for the class description was the Land Cover Classification System (LCCS) [25,26]. Table 3 gives an overview on the target classes, their LCCS description and coding as well as the respective classifiers.

The legends of the LULC products are marked by their different class depths and class definitions. In order to be able to compare the thematic information, the legends must be harmonized [27, 28]. The harmonization result showed that a definite class assignment was not always possible, due to variant specifications in the used literature and the range of interpretation for the class definitions. This was especially the case for mosaic classes, which unite different land cover and land use types with same proportions in a single class. Since these classes have a significant share in the investigated area, the assignment to the target classes was made by a cross comparison with the National Land Cover Dataset (NLCD) of China [29]. According to the distribution of the mosaic classes to the respective NLCD classes, the dominant class fraction was defined as the target class. The error introduced during harmonization conditioned by ambiguous class assignments was neglected because an explicit definition was necessary.

Based on the harmonized and re-classified LULC products, the inter-comparison with the SAR-based GSV products was applied. As a result, we used the distribution of the GSV values with respect to each of the four defined target classes for the definition of a threshold to distinguish forest related and non-forest related GSV values. Figure 1 shows an example of the inter-comparison with respect to the Envisat ASAR GSV product for Northeast China. While for forest, the GSV was mostly typical of mature forest, for cropland, a certain amount of pixels were classified having a GSV between 50 and 100 m^3/ha. The intersection of both distribution functions was used to define the GSV forest/non-forest threshold, which in turn helped to tune the BIOMASAR algorithm with respect to the range of GSV that can be retrieved. This resulted in more accurate definitions of GSV levels for forest/non-forest distinction, particularly in transition regions between forest and shrubland.

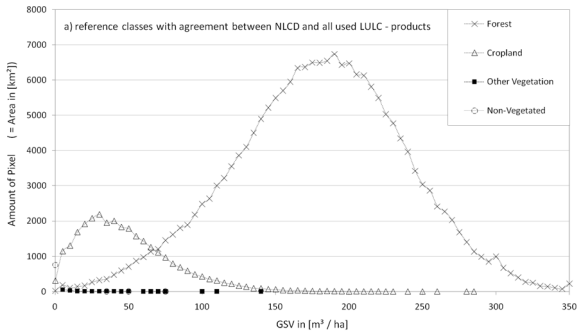

Figure 1. Distribution of the GSV estimated from Envisat ASAR images for the four target classes in Northeast China.

Figure 2 shows the classification of the ERS1/2 GSV product into forest/non-forest as well as specific areas, which were masked out using the cropland information of the GLC2000 product. These masked areas are characterized by intensive rice cultivation (e.g. Sichuan province), which leads to misclassifications in the ERS GSV product due to the SAR specific backscatter characteristic. The application of the cropland information extracted from the LULC products significantly improved the quality of the respective GSV based forest/non-forest classification (increase of overall accuracy up to 7 %).

Table 2. Freely available global LULC products used in this study

	Product (Version)	Satellite/ Sensor (Acquisition period)	Source
Time Period 1	UMD	NOAA-AVHRR (Apr ´92-Mar´93)	http://glcf.umiacs.umd.edu/data/landcover/index.shtml
	GLCC (V002)	NOAA-AVHRR (Apr´92-Mar´93)	http://LPDAAC.usgs.gov/glcc/ea_int.html
Time Period 2	GLC2000	SPOT-VGT (Nov´99-Dec´00)	http://www-gem.jrc.it/glc2000
	MODIS ´01 (V004)	TERRA-MODIS (Jan´01-Dec´01)	https://lpdaac.usgs.gov/lpdaac/get_data/data_pool
Time Period 3	GlobCover´05 (V02.2)	ENVISAT- MERIS (Dec´04-Mar´06)	http://ionia1.esrin.esa.int/index.asp
	MODIS ´05 (V005)	TERRA-MODIS (Jan´05-Dec´05)	https://lpdaac.usgs.gov/lpdaac/get_data/data_pool

Table 3. Specifications of the defined target classes according to the LCCS.

Class Name	***LCC Code*** *LCC Formula*	***LCC Label*** *(Explanatory Notes)*
forest	10001 // 21441 // 21445 // 3403// 41519 // 41635 A1 // A1A20 // A3A20 // A3 // A1A20 // A3A20	Tree Crop(s) // Closed to Open Woody Vegetation // Closed to Open Trees // Woody Crops // Closed to Open Woody Vegetation // Closed to Open Trees *(Tree / Canopy Cover > 10 %, Height > 2 m, dominated amount of area)*
cropland	10037 // 3001 A4 // A1	Graminoid Crop(s) // Graminoid Crops *(Cropland Cover > 50 %)*
other vegetation	0004 // 0007 A12 // A24	Natural and Semi-Natural Primarily Terrestrial Vegetation // Natural and Semi-Natural Aquatic or Regularly Flooded Vegetation *(NOT "forest" or "cropland", dominated amount of area)*
non-vegetated	0010 // 0011 // 0013 // 0014 B15 // B16 // B27 // B28	Artificial Surfaces and Associated Area(s) // Bare Area(s) // Artificial Water bodies, Snow and Ice // Natural Water bodies, Snow and Ice

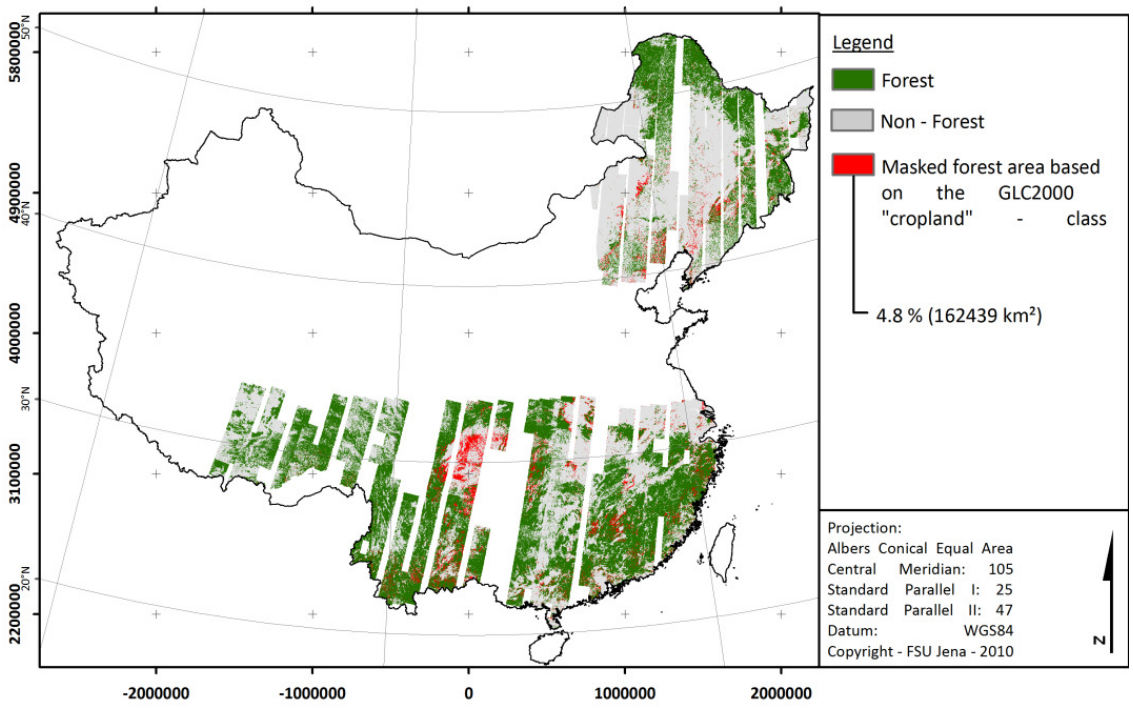

Figure 2. Forest/non-forest classification based on the ERS-1/2 GSV product and masked agriculture areas (red) based on the LULC information of GLC2000.

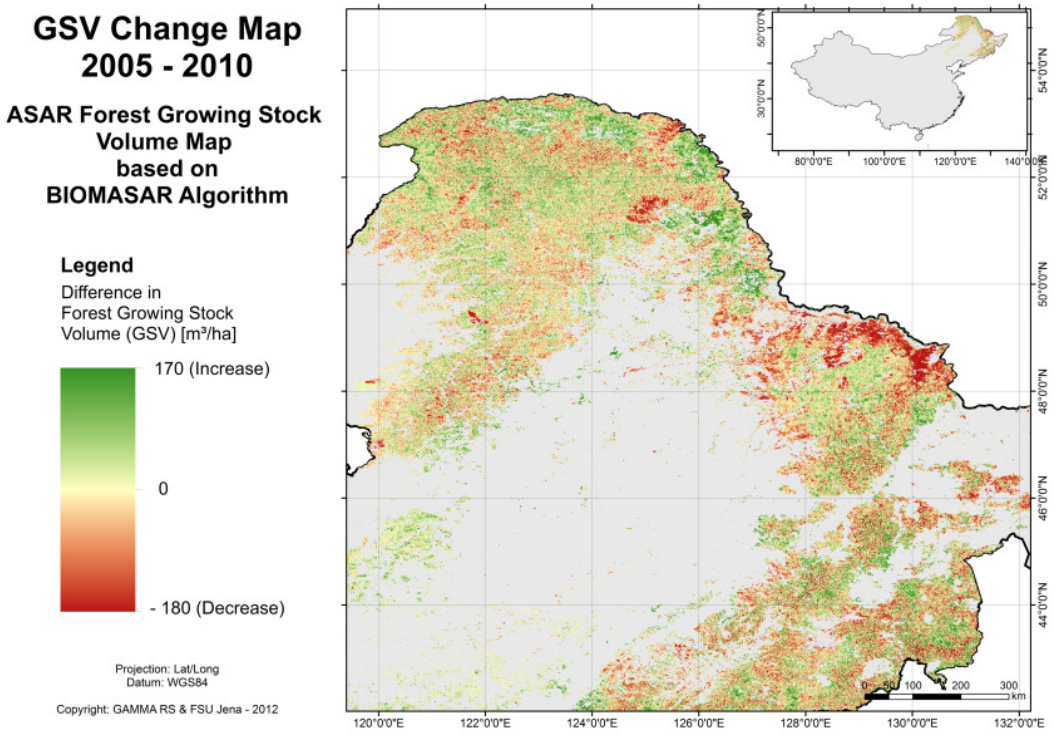

Figure 3. GSV change map from GSV estimates obtained with the BIOMASAR algorithm using Envisat ASAR ScanSAR images acquired in 2005 and 2010.

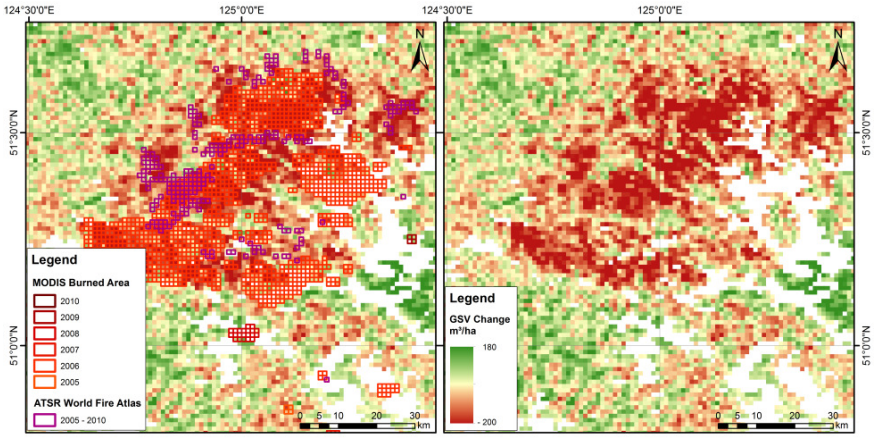

Figure 4. MODIS Burned Area and ATSR World Fire Atlas overlaid on the GSV change map (left) and GSV change map (right) for a fire detected in 2006.

4. GSV CHANGE BETWEEN 2005 AND 2010

The Envisat ASAR GSV maps for the years 2005 and 2010 were used to analyze the GSV change in Northeast China (Figure 3). In particular, it was attempted to distinguish between loss of GSV due to fire and clear-cutting activities. Increase of GSV was checked for plausibility. The study area has a total coverage of about 540.000 km² including forest and shrubland areas according to the GLC2000 dataset. The forest is characterized by several changes through fire, logging, clear-cutting and re- and afforestation.

The GSV estimated with the BIOMASAR algorithm presents an uncertainty quantified on the order of 10% regardless of the GSV level [5]. Hence. an analysis was done to assess the influence of the 10% uncertainty of the GSV values on the detected changes. From the 2005 and 2010 GSV maps, 100 simulations were carried out including random Gaussian distributed errors according to the standard deviation of the value (10%). The results show that there is an influence of the uncertainty, but the change map detects increase and decrease areas almost correctly for high GSV values. The absolute value of the change may not be precise due to the 10% uncertainty. Nevertheless the tendency of increase or decrease seems to be correct. The analysis also took into account that GSV estimates based on less than 20 measurements of the SAR backscatter could present significant errors [5]. These pixels often exist in areas with steep topography. Results are here presented considering all GSV estimates and only those based upon at least 20 backscatter measurements.

To verify whether changes of GSV could be explained as a consequence of fire events, the GSV change map was compared with the MODIS Burned Area Product [14] and ATSR World Fire Atlas [13] between 2005 and 2010. Figure 4 shows an example of GSV decrease in correspondence of a large fire detected by the EO-based fire products in 2006. Further insight on the consistency between EO-based fire products and the GSV change map is provided by the histogram in Figure 5. The GSV change was grouped into classes with negative values corresponding to GSV decrease and positive values corresponding to GSV increase. Areas detected as affected by fire are characterized by GSV decrease. For about 40% of such areas the corresponding GSV change was below the level that could be considered detectable with the BIOMASAR algorithm and C-band backscatter data. Some areas presented an increase of more than 25 m^3/ha, i.e. more than the intrinsic uncertainty in the GSV change estimates. It is unclear whether the discrepancy could be due to an error in the EO-based fire products or in the GSV estimates. Further investigation on this topic shall include an assessment of degree of consumption of the canopy/trunk due to the fire.

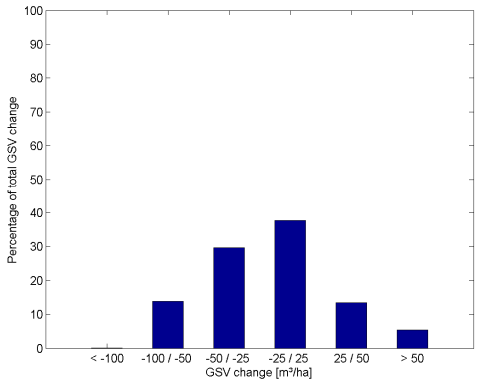

Figure 5. Histogram of GSV change in areas affected by fire according to the MODIS Burned Area Product [14] and ATSR World Fire Atlas [13] between 2005 and 2010.

Possible effects of clear-felling activities were observed in the East of the Xunke Country and in the North of the Yichun District. While the GSV presented large decrease, the EO fire products did not show any detection of fire. To assess whether the GSV decrease was due to clear-cut, the variation of the Short Wave Infrared (SWIR) band in Landsat images were considered. In [30], it was shown that a burned area can be distinguished from a clear cut area with the help of the Landsat SWIR band. A large difference in fire and clear-cut response in the SWIR band can be recognized after about 3-4 years after the disturbance. The most suitable Landsat dataset over the area of interest consisted of two images acquired in 2000 and 2006. Figure 6 shows that the area characterized by strong decrease of GSV was also characterized by large variation of the SWIR band. Similar results were obtained for the Northeast of the Heilongjiang Province.

To assess the plausibility of GSV increase estimated from the two ASAR GSV maps, yearly growth rate of the forest in Northeast China and uncertainty of the GSV estimates had to be taken into account. For the study area, the yearly growth rate was assumed between 5 and 10 m³/ha/year. Hence, for the five years interval between the acquisition of the ASAR data used to obtain the GSV maps for 2005 and 2010, the forest could not grow more than 50 m³/ha. To quantify the areas showing an unrealistic increase, the 10% uncertainty were subtracted from or added to the GSV map of 2005 and 2010, respectively. Thus the case of maximum GSV increase is assumed. As a result of these assumptions, we concluded that no significant increase was detected for GSV change below 25 m³/ha. GSV increase in the range of 25 and 50 m³/ha was realistic (depending on the forest type). Finally, an increase greater than 50 m³/ha was assumed to be unrealistic.

Figure 7 shows the GSV change map grouped into four classes according to the levels of realistic/unrealistic increase. About 86% of the areas for which GSV was found to increase between 2005 and 2010 presented an increase within a natural range of values. After removal of the estimates based on less than 20 backscatter observations, about 88 % of the increasing areas were within a natural range. Some patches in the Southeast of the study area show a high increase caused maybe by re- or afforestation areas [31]. Unrealistic increase of GSV was identified in five areas located in the Northeast of the Heilongjiang Province. Three of these were affected by fires before 2005 (Mohe, 1987 [32], Tahe, 2003 and Huma, 2003). There are several ways a forest can react after a fire disturbance. Forest stands have naturally fast increase of GSV a few years after fire disturbance [33]. This can result in a much higher GSV increase than 10 m³/ha/year. Unfortunately these areas cannot be confirmed by MODIS VCF tree canopy cover estimates between 2005 and 2010, which is showing just a little or no increase of percentage tree cover.

Overall statistics of area and volume based on the GSV change estimates indicate that forest resources of Northeast China decreased slightly between 2005 and 2010 (Table 4). The statistics consider all forest and shrubland pixels according to the GLC2000 land cover product, and GSV estimates based upon at least 20 backscatter measurements (420,501 km^2). For 298,844 km^2, i.e., 71% of pixels, the detected change was below the uncertainty margin of a GSV estimate. Notwithstanding changes less than 25 m^3/ha, the decrease of GSV was primarily in the range between 25 to 50 m^3/ha. Changes corresponding to a decrease of over 100 m^3/ha were rare. GSV increase was for 98.6% of the study area below 50 m^3/ha (84% below 25 m^3/ha). Regardless whether changes below the 25 m^3/ha are considered or not, the area characterized by GSV decrease was larger than the area characterized by GSV increase. Accordingly, the loss of volume exceeded the increment over the five years. The GSV change map between 2005 and 2010 indicates a net loss of volume of 12,122 m^3 (8,069 m^3 for changes greater than 25 m^3/ha).

Table 4. Overall statistics of changes derived from GSV change map in Figure 3.

	Area [km²]	Volume [m³]
Decrease of GSV		
0-25 m³/ha	183,157	-19,507
25-50 m³/ha	45,550	-15,367
50-100 m³/ha	5,869	-3,482
> 100 m³/ha	7	-8
Total	**234,582**	**-38,363**
Total (> 25 m^3/ha)	**51,426**	**-18,857**
Increase of GSV		
0-25 m³/ha	155,327	15,453
25-50 m³/ha	28,131	9,343
>50 m³/ha	2,461	1,445
Total	**185,919**	**26,241**
Total (> 25 m^3/ha)	**30,592**	**10,788**
Total GSV Change	**420,501**	**-12,122**
Total GSV Change (> 25 m^3/ha)	**82,018**	**-8,069**

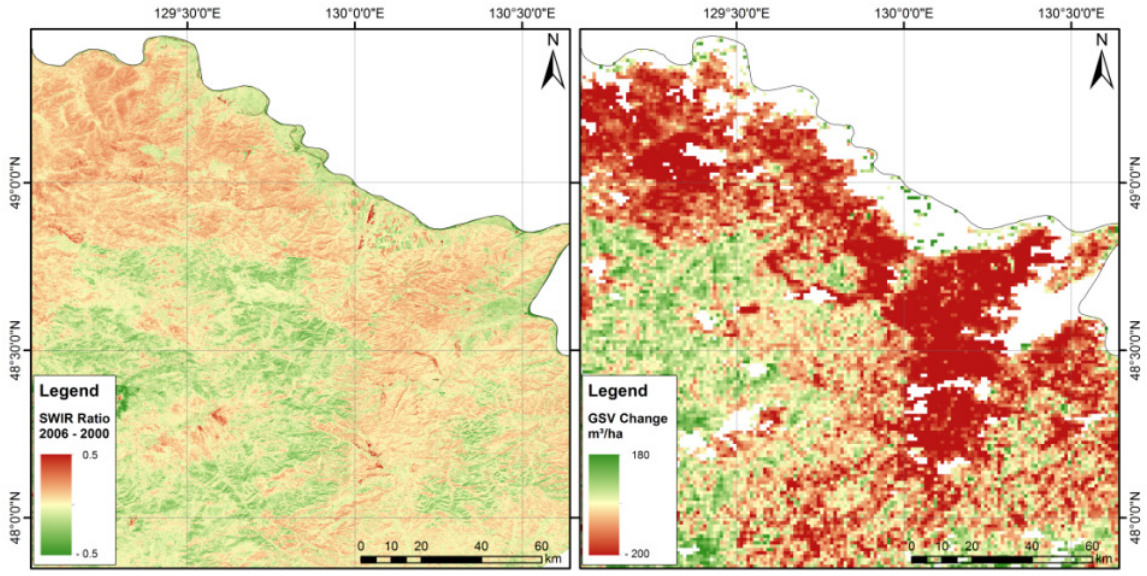

Figure 6. SWIR ratio of Landsat images acquired in June 2000/2001 (ETM+) and September 2006 (TM) (left) and corresponding GSV change detected in Envisat ASAR images (right). A positive SWIR ratio (red tones) corresponds to strong decrease of GSV between 2005 and 2010, i.e. negative GSV change (red tones).

\

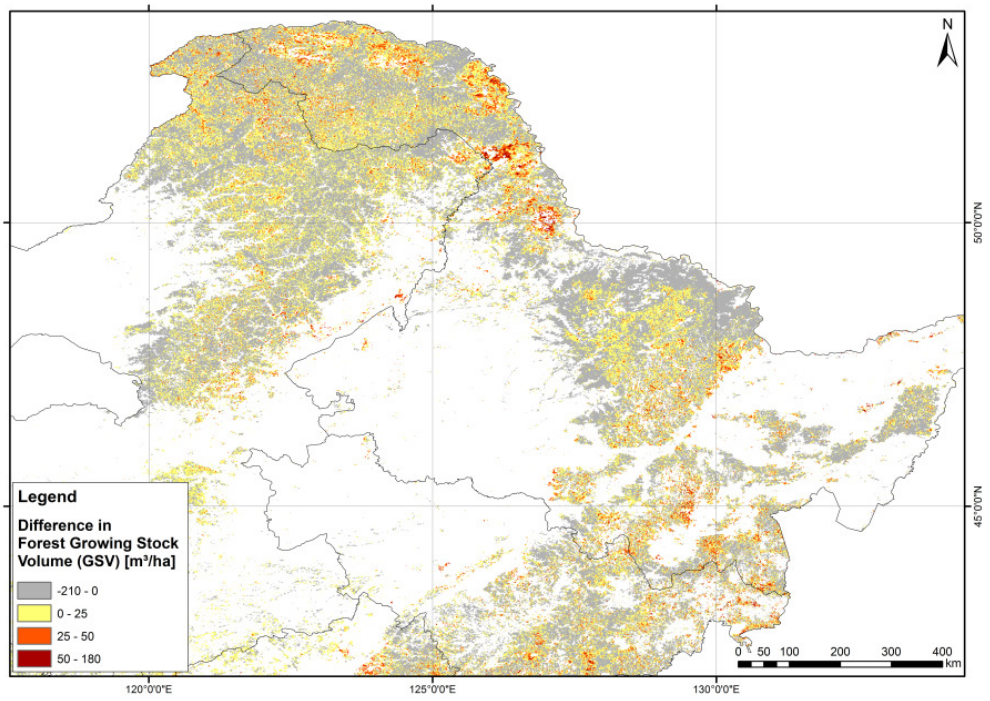

Figure 7. GSV change map coded into four classes to highlight realistic and unrealistic GSV increase.

5. ACKNOWLEDGMENTS

ESA and MOST are greatly acknowledged for establishing and managing the DRAGON and DRAGON 2 Programme. All Forest DRAGON project partners are acknowledged for cooperation. ERS data were available through ESA Dragon AO Category 1 Project 2583. The GSV estimates from Envisat ASAR ScanSAR were obtained within ESA's STSE BIOMASAR-II project. Processing of the Envisat ASAR data acquired in 2010 was carried out on the Grid Processing on Demand (G-POD) platform at ESA. Access to G-POD was granted through Cat.1 Proposal 8525.

6. REFERENCES

1. Cartus, O., M. Santoro, C. Schmullius, Y. Pang, E. Chen & Z. Li (2008): Creation of Large Area Forest Biomass Maps For Northeast China using ERS-12 Tandem Coherence. Proc. Dragon 1 Programme Final Results 2004-2007. Beijing, P. R. China. ESA-SP 655, April 2008.
2. Schmullius, C., Reiche, J., Leiterer, R., Cartus, O., Santoro, M., Wegmüller, U., Li, Z., Tian, X. & Ling, F. (2010). FOREST DRAGON 2: Mid-term results of the European partners. In Proc. Symposium Dragon 2 Programme Mid-Term Results 2008-2010 (Eds. H. Lacoste-Francis), ESA Communications, ESTEC, Nordwijk, The Netherlands, SP-684, CD-ROM.
3. Cartus, O., Santoro, M., Schmullius, C. & Li, Z. (2011). Large area forest stem volume mapping in the boreal zone using synergy of ERS-1/2 tandem coherence and MODIS vegetation continuous fields. *Remote Sens. Environ.* **115**(3), 931-943.
4. Xin, T., Li, Z., Chen, E., Yong, P., Yongtian, Y., Schmullius, C., Cartus, O., Santoro, M. & Le Toan, T. (2008). Large-scale forest mapping in northeast China and map updating by using ERS-1/2 tandem and Envisat ASAR data. In Proc. Dragon 1 Programme Final Results 2004-2007 (Eds. H. Lacoste & L. Ouwehand), ESA Communication Production Office, ESTEC, Nordwijk, The Netherlands, SP-655, CD-ROM.
5. Santoro, M., C. Beer, O. Cartus, C. Schmullius, A. Shvidenko, I. McCallum, U. Wegmüller, A. Wiesmann (2011): Retrieval of growing stock volume in boreal forest using hyper-temporal series of Envisat ASAR ScanSAR backscatter measurements. *Remote Sens. Environ.* **115** (2), 490-507.
6. Utoltsev, V.A. (2010): Eurasian Forest Biomass and Primary Production Data. Yekaterinburg: Ural Branch of Russian Academy of Sciences, 2010.
7. Luyssaert S., I. Inglima & M. Jung et al. (2007): The CO2-balance of boreal, temperate and tropical forest derived from global database. *Global Change Biology* **13**, 2509-2537.
8. SFA (State Forestry Administration) (2002): China forestry statistical yearbook 2002. Beijing: China Forestry Publishing House.
9. Kindermann, G.E., I. McCallum, S. Fritz & M. Obersteiner (2008): A Global Growing Stock, Biomass and Carbon Map Based on FAO Statistics. *Silva Fennica* **42** (3), 387-396.
10. Simard, M., N. Pinto, J.B. Fisher & A. Baccini (2011): Mapping forest canopy height globally with spaceborne lidar. Journal of Geophysical Research - Biogeosciences **116**, G04021, 1-12.
11. Carroll, M.L., C.M. DiMiceli, R.A. Sohlberg, and J.R.G. Townshend (2004): 250m MODIS Normalized Difference Vegetation Index, 250ndvi28920033435, Collection 4, University of Maryland, College Park, Maryland, Day 289, 2003. (digital data accessed 05/13/2012 from <http://reverb.echo.nasa.gov/reverb>).
12. Giglio, L., Descloitres, J., Justice, C.O., Kaufman, Y. (2003): An enhanced contextual fire detection algorithm for MODIS. *Remote Sens. Environ.* **87**, 273-282.
13. Arino O., S. Casadio & D. Serpe (2012): Global night-time fire season timing and fire count trends using the ATSR instrument series. *Remote Sens. Environ.* **116**, 226-238.
14. Boschetti, L., D. Roy & A. A. Hoffmann (2009): MODIS Collection 5 Burned Area Product – MCD45, User Guide Version 2.0.
15. Hansen, M., R.S. DeFries, J.R.G. Townshend, M. Carroll, C. Dimiceli, and R.A. Sohlberg (2003): Global Percent Tree Cover at a Spatial Resolution of 500 Meters: First Results of the MODIS Vegetation Continuous Fields Algorithm. *Earth Interactions* **7** (10), 1-15.
16. Townshend, J.R.G., M. Carroll, C. Dimiceli, R. Sohlberg M. Hansen & R. DeFries. (2011): Vegetation Continuous Fields MOD44B, 2001 Percent Tree Cover, Collection 5, University of Maryland, College Park, Maryland, 2001. (digital data accessed 05/13/2012 from <http://reverb.echo.nasa.gov/reverb>).
17. Urban, M., S. Hese, M. Herold, S. Pöcking & C. Schmullius (2010): Pan-Arctic Land Cover Mapping and Fire Assessment for the ESA Data User Element Permafrost. PFG 4, 283 -293.
18. Bartholome, E. & A. Belward (2005): GLC2000: A new approach to global land cover mapping from Earth observation data. *Int. J. Remote Sens.* **26** (9), 1959-1977.
19. Friedl, M.A., D. Sulla-Menashe, B. Tan, A. Schneider, N. Ramankutty, A. Sibley & X. Huang (2010): MODIS Collection 5 global land cover: Algorithm refinements and characterization of new datasets. *Remote Sens. Environ.* **114** (1), 168-182.

20. Degree Confluence Project (digital data accessed 03/12/2012 from <http://confluence.org/>).
21. University of Oklahoma (2011): A Library of Georeferenced Photos from the Field. - AGU, EOS, 12/6/2011.
22. Rabus, B., Eineder, M., Roth, A. & Bamler, R. (2003). The Shuttle Radar Topography Mission - a new class of digital elevation models acquired by spaceborne SAR. *ISPRS Journal of Photogrammetry & Remote Sensing* **57**, 241-262.
23. NASA Landsat Program (2003): Landsat ETM+, Surface Reflectance, USGS, Sioux Falls, 16/06/2000.
24. Open Geospatial Consortium Inc. (2006): OpenGIS® Web Map Server Implementation Specification. OGC 06-042.
25. Ahlqvist, O. (2008). In search for classification that support the dynamics of science - The FAO Land Cover Classification System and proposed modifications, *Environment and Planning B: Planning and Design* **35** (1), 169-186, 2008.
26. Di Gregorio, A. & Jansen, L.J.M. (2005). Land Cover Classification System (LCCS): Classification Concepts and User Manual, Software Version 2, FAO, Rome, Italy, 191 p., 2005.
27. Herold, M., Woodcock, C., Di Gregorio, A., Mayaux, P., Belward, A.S. & Latham, J. (2006). A Joint Initiative for Harmonization and Validation of Land Cover Datasets, *IEEE Trans. Geosci. Remote Sensing* **44** (7), 1719-1727.
28. Jansen, L.J.M., Groom, G. & Carrai, G. (2008). Land-cover harmonisation and semantic similarity: some methodological issues, *Journal of Land Use Science* **3** (2), 131-160.
29. Liu, J., Liu, M.L., Tian, H.Q., Zhuang, D.F., Zhang, Z.X., Zhang, W., Tang, X.M. & Deng, X.Z. (2005). Spatial and temporal patterns of China's cropland during 1990-2000. An analysis based on Landsat TM data, Remote Sensing of Environment, 98, 442-456.
30. Schroeder, T.A., Wulder, M.A., Healey, S.P. & Moisen, G.G. (2011). Mapping wildfire and clearcut harvest disturbances in boreal forests with Landsat time series data. *Remote Sens. Environ.* **115**, 1421-1433.
31. Yu, D.Y., Shi, P.J., Han, G.Y., Zhu, W.Q., Du, S.Q. & Xu, B. (2011). Forest ecosystem restoration due to a national conservation plan in China, *Ecological Engineering* **37**, 1387-1397.
32. Qu, J. J., HAO, X., Liu, Y., Riebau, A.R., Yi, H. & Qin, Y. (2009). Remote Sensing Applications of Wildland Fire and Air Quality in China. In: Bytnerowicz, A., Arbaugh, M. Riebau, A.R. & Andersen C. (Editors): Developments in Environmental Science, 8, 277-288.
33. Seedre, M., Shresthra, B.M., Chen, H.Y.H., Colombo, S. & Jögiste, H. (2011). Carbon dynamics of North American boreal forest after stand replacing wildfire and clearcut logging, *Journal of Forest Resources* **16**, 168-183.